Academic Journal of Science and Technology
ISSN: 2771-3032 | Vol. 2, No. 2, 2022

Numerical Simulation of Initial Residual Stress in Thermal Barrier Coatings: Planar geometry model

Qixing Liu[1, a]

[1]Zhuzhou Times New Material Technology CO., LTD, Zhuzhou, Hunan, 412007, China
[a]Liuqx2@csrzic.com

Abstract: Thermal barrier coatings (TBCs) are one of the key materials of turbines for propulsion and power generation. A typical TBCs system generally contains four layers, i.e. top ceramic coat (TC), thermally grown oxide (TGO), bond coat (BC) and substrate. The material parameters （such as Young's modulus, Poisson's ratio and thermal expansion coefficient） of each layer will result in the different cooling velocity of thermal barrier coatings (TBCs) system during the deposition process. Initial residual stresses in TBCs occur after cooling to the ambient, which play an important role for evaluating the failure and reliability of TBCs. In this paper, the initial residual stresses of a planar TBCs model were obtained by finite element method, the effects of cooling kinds and the thickness of TC and TGO on the fields of initial residual stresses were also considered. The results may be useful for the optimization of TBCs system design and preparation.

Keywords: Thermal barrier coatings, Initial residual stress, Finite element method.

1. Introduction

With the development of gas turbine to high inlet temperature, the traditional nickel-based and cobalt-based superalloys, directional crystalline alloys and even single crystal alloys can no longer fully meet the requirements of high-temperature components of gas turbine, and the use of air cooling systems and cooling channel improvements can only obtain limited cooling effect, in this case, thermal barrier coatings (abbreviated as TBCs) came into being. Thermal barrier coating is a ceramic coating, which is one of the key technologies for modern aero engines. The thermal barrier coating system is a typical multi-layer structure system, mainly consisting of a ceramic layer abbreviated as TC), Thermally grown oxide (abbreviated as TGO), Bond coat (abbreviated as BC) and Substrate, etc. Four layers of materials are composed. Thermal barrier coatings can effectively reduce the temperature of the protected substrate in service, reduce its thermal shock load, reduce the need for cooling air, and improve the thermal efficiency of the device, thus being widely used in aerospace, chemical, metallurgical and energy fields [1-4].

The formation of initial residual stresses within a thermal barrier coating system is a complex process, and many factors such as the material composition, thickness, and coating temperature of the substrate and each coating determine the final residual stress distribution. Although there are many sources of residual stresses in thermal barrier coatings, they are mainly caused by the mismatch between the thermal expansion of the coating and the substrate, which have formed a solid, when they cool down from the high temperature internal stress-free state to room temperature [5-6]. In the actual preparation process, due to the mismatch problem of elastic modulus, Poisson's ratio, thermal expansion coefficient and thermal conductivity of each layer of the thermal barrier coating system, it will lead to different cooling rates of each layer of the material in its body, and after the preparation is completed, eventually there are thermal residual stresses in each layer of the thermal barrier coating system after cooling to room temperature. During the service life of a thermal barrier coating system, these thermal residual stresses have a very important impact on its lifetime [7-8]. The influence of these thermal residual stresses remaining during the preparation process must also be considered in the theoretical work on the prediction of the lifetime of thermal barrier coatings.

Mao Weiguo et al. obtained the analytical solution expressions for the thermal residual stresses in each layer of the flat model thermal barrier coating system and analyzed the effects of the cooling method and ceramic coating thickness on the residual stresses in each layer [7]. Harding et al. proposed an improved analytical model for the deposition process of thermal barrier coatings that can take into account the microstructure of the coating as well as the influence of some preparation parameters [9]. Teixeira et al. investigated the residual stresses in the preparation of thermal barrier coatings using both X-ray and numerical simulation methods and found that the residual stresses in the coatings would change from tensile to compressive stresses as the substrate temperature increased[10]. The initial residual stresses in the three-layer flat plate model thermal barrier coating system were obtained by Widjaja et al. using the finite element method[11]. Among these research works, few studies have considered both the integrity of the thermal barrier coating system and the inhomogeneity of the stress analysis within each layer as well as the effect of interfacial oxidation on the initial residual stress during preparation.

In this paper, we mainly apply the finite element method, and in the first part we first consider the displacement and stress distribution within the thermal barrier coating system during the cooling process after the preparation is completed, assuming that the temperature of each layer is cooled from 800°C to 1600°C to room temperature as a whole, respectively, and the displacement and stress distribution within the thermal barrier coating system is analytically obtained. Then the effects of the thickness of the TGO (0.5 μm-8 μm) and the thickness of the TBC (0.1 mm-0.9 mm) formed during the preparation process on the initial residual stress distribution were examined separately. The second part of this paper focuses on the thermal barrier coating system of

the flat plate model when cooling is completed after preparation, assuming that a temperature gradient exists for each layer. That is, the TGO, BC and substrate temperatures are all fixed at 800°C. The distribution of the initial residual stresses when the ceramic coating is cooled from different temperatures (800°C-1600°C) to room temperature.

2. Finite Element Analysis Model

2.1. Geometric Model

In general, thermal barrier coating systems generate a thin TGO layer between the TBC and BC second layers during the preparation process and after thermal cycling. With the growth of service time, TGO will continue to thicken and its maximum thickness can reach 20μm [12]. After considering the generation of TGO layer, the thermal barrier coating system is a four-layer structure, namely TBC, TGO, BC and substrate, and the schematic diagram of its flat plate model is shown in Figure 1. The thickness direction of the system is 2-way. Where h_c , h_t, h_b, h_s are the thickness of TBC, TGO, BC and substrate respectively. The size of each layer thickness: h_c =0.35mm, h_t=0.50μm, h_b=0.1mm, h_s =2.0mm [7, 13]. Length of the model:L=10mm. When the thermal barrier coating system is in service, the upper surface of the TBC is in contact with the high temperature environment with high temperature heat flow, and the lower surface of the substrate is the inner wall of the cooling channel, where the cooling medium takes the heat away continuously, thus reducing the temperature.

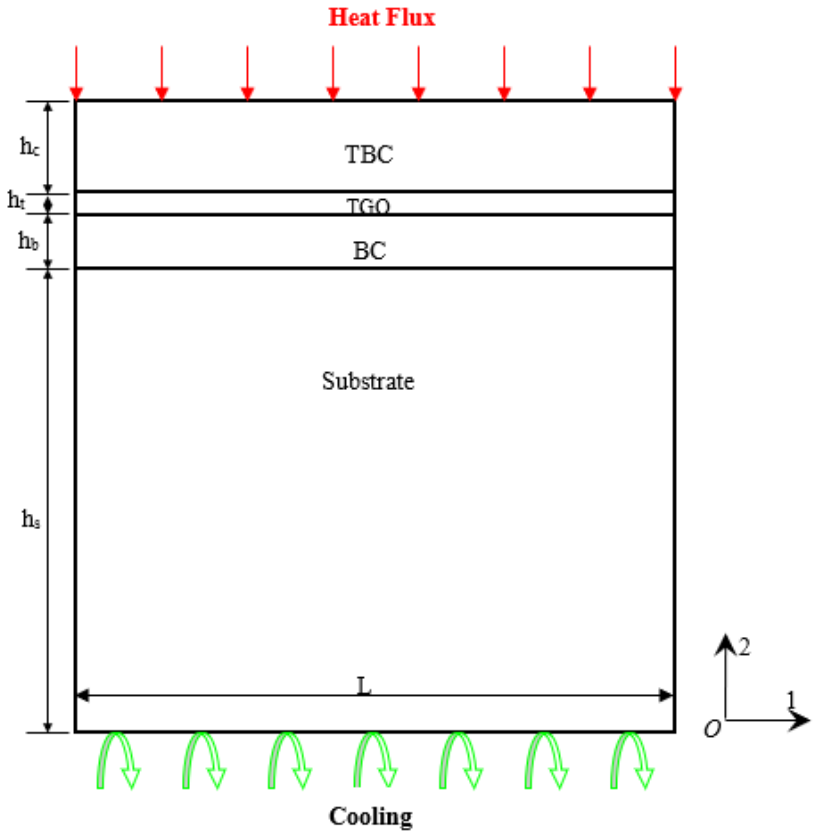

Figure 1. The tablet model of 4-Layer TBCs

2.2. Material Parameters

In this paper, the material parameters provided in the literature [14-15] are chosen. The parameters such as thermal conductivity, modulus of elasticity, Poisson's ratio, and coefficient of thermal expansion are temperature dependent. As shown in Tables 1-6. In this paper, the yielding and creep phenomena of the layers of the material during the cooling process after the preparation is completed are not considered.

Table 1. Thermal conductivity

Temperature(°C)	SUB(W/m°C)	BC(W/m°C)	TGO(W/m°C)	TBC(W/m°C)
20	88.000	5.800	10.000	1.956
200	73.300	7.500	7.794	1.834
400	59.500	9.500	6.029	1.736
600	62.000	12.000	5.074	1.627
800	65.000	14.500	4.412	1.634
1000	68.100	16.200	4.412	1.681
1100	69.000	17.000	4.000	1.700

Table 2. Young's modulus

Temperature(℃)	SUB(GPa)	BC(GPa)	TGO(GPa)	TBC(GPa)
20	220	200	400	48
200	210	190	390	47
400	190	175	380	44
600	170	160	370	40
800	155	145	355	34
1000	130	120	325	26
1100	120	110	320	22

Table 3. Poisson's ratio

Temperature (℃)	SUB	BC	TGO	TBC
20	0.31	0.30	0.23	0.10
200	0.32	0.30	0.23	0.10
400	0.33	0.31	0.24	0.10
600	0.33	0.31	0.24	0.11
800	0.34	0.32	0.25	0.11
1000	0.35	0.33	0.25	0.12
1100	0.35	0.33	0.25	0.12

Table 4. Specific heat

SUB $(J/Kg \cdot K)$	BC $(J/Kg \cdot K)$	TGO $(J/Kg \cdot K)$	TBC $(J/Kg \cdot K)$
440	450	755	505

Table 5. Density

SUB (Kg/mm^3)	BC (Kg/mm^3)	TGO (Kg/mm^3)	TBC (Kg/mm^3)
8500	7380	3984	3610

Table 6. Coefficient of thermal expansion

Temperature (^oC)	SUB($*10^{-6}/^oC$)	BC($*10^{-6}/^oC$)	TGO ($*10^{-6}/^oC$)	TBC($*10^{-6}/^oC$)
20	14.8	13.6	8.0	9.0
200	15.2	14.2	8.2	9.2
400	15.6	14.6	8.4	9.6
600	16.2	15.2	8.7	10.1
800	16.9	16.1	9.0	10.8
1000	17.5	17.2	9.3	11.7
1100	18.0	17.6	9.6	12.2

2.3. Boundary Conditions

In order to make the finite element model not move and rotate during the calculation, we set the mechanical boundary conditions as follows:

Lower left corner at A.:u_1=u_2=0. Where 1 and 2 denote the displacement components along the 1 and 2 directions, respectively;

Lower right corner at B. : u_2=0. The boundary conditions are set as shown in Figure 2.

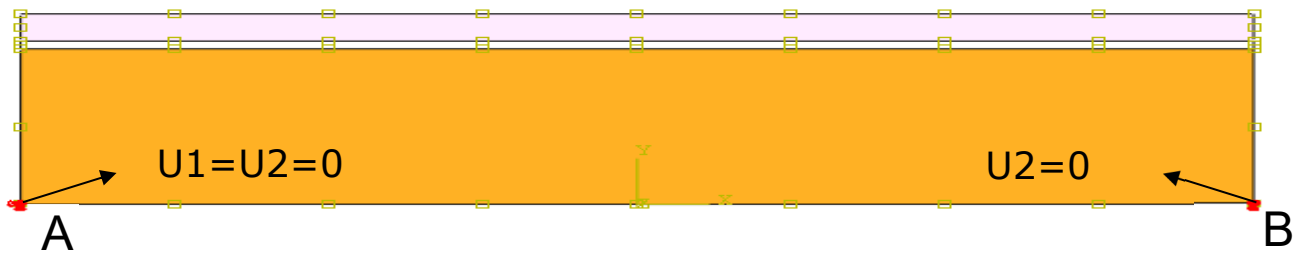

Figure 2. Boundary conditions

2.4. Grid Division

The mesh division of the model is shown in Figure 3. (a) Since the thickness of TGO is small, but its stress value is often large, we have especially refined the mesh of TGO. Since the substrate is relatively thick and is not the focus of our investigation, the substrate is meshed more coarsely. This can reduce the amount of computation while ensuring a

certain level of computational accuracy. We used CPE4RT type cells, with a total of 22317 cells used.

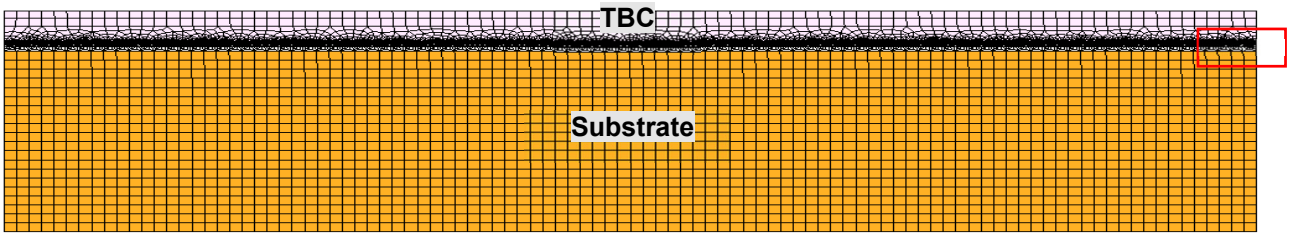

Figure 3. Meshes

3. Cooling Method I: Cooling from The Same Temperature of The Thermal Barrier Coating System to Room Temperature

First, assuming that the layers of the thermal barrier coating system are uniformly cooled to room temperature as a whole after deposition from the preparation temperature, we choose a preparation temperature of 800℃~1600℃ [7].

3.1. h_c =0.35mm, h_t =0.5μm

We first focus on the thickness of the ceramic layer when h_c =0.35mm. Thickness of oxide layer h_t =0.5μm. The situation when the preparation temperature is 800°C. When the thermal barrier coating system is prepared and the whole is uniformly cooled to room temperature, the displacement distribution of the system is shown in Figure 4. Figure 4(a) shows the distribution of the total displacement magnitude, and Figure 4(b) shows the distribution of the displacement components in the thickness direction. Due to the boundary conditions, the system shrinks with the lower left corner endpoint (point A) as the center during the cooling process. The displacement at the upper right corner is the largest, about 0.127mm. The displacement component in the thickness direction is non-uniform and the system undergoes upward bending.

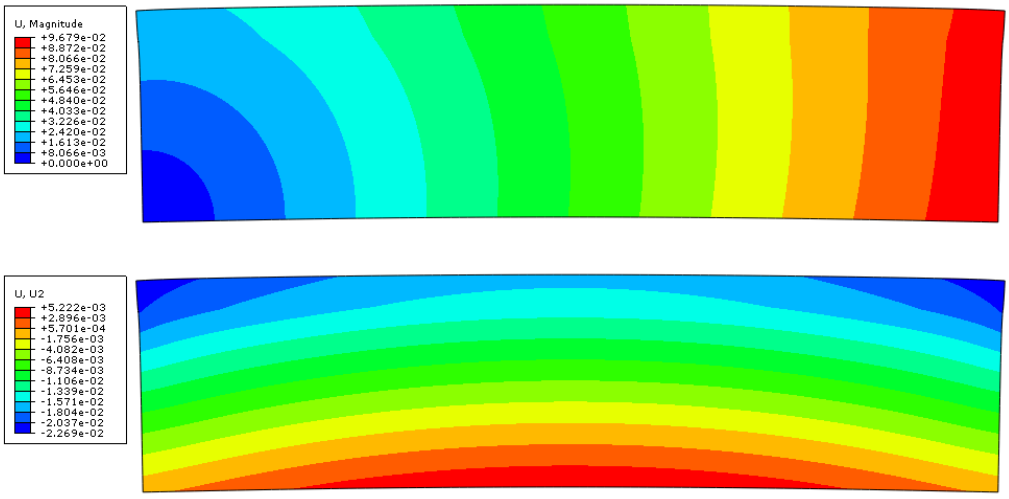

Figure 4. Displacement distributions

Figure 5 represents the σ_{11} distribution cloud within the system, from which we can see that the σ_{11} distribution within each layer is non-uniform, with a large stress and its gradient in the boundary region and a more uniform stress distribution near the middle.

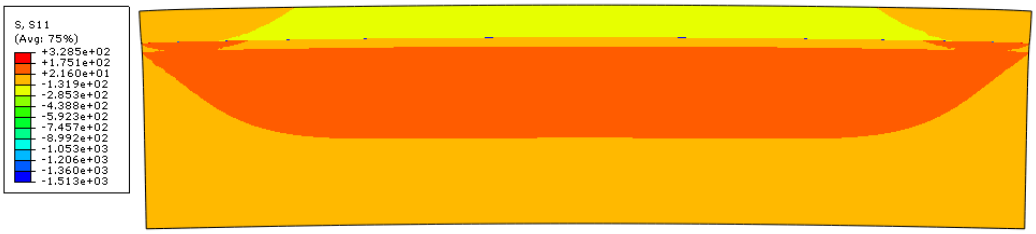

Figure 5. Distributions of S11

In order to quantitatively represent the distribution of σ_{11} within the TBC, we selected 3 analysis paths within the TBC, which are the upper surface, lower surface and $h/2$ middle surface of the TBC. The σ_{11} distributions on the selected 3 paths are shown in Figure 6. As can be seen from the figure, most of the area within the TBC is under compressive stress, and only a small area at the diametral boundary on the upper surface is under tensile stress. The stress distribution in the horizontal direction within the TBC is non-uniform, with the stress at the two end boundaries being small, tending to 0 MPa,

and the stress in the middle being large, with a stress value of about -135 MPa. In the thickness direction, the closer to the upper surface, the lower the stress, but the gradient of variation is small. In the middle part of the TBC, the σ_{11} at the interface with the TGO is about 20 MPa higher than the stress value near the upper surface. The dotted line in Figure 6 indicates the results of the analytical solution [7], which assumes a uniform stress distribution within the coating. the stress distribution in the middle part of the TBC is closer to the analytical solution, and if the effect of the boundary is not considered, the finite element results are in good agreement with the results of the analytical solution.

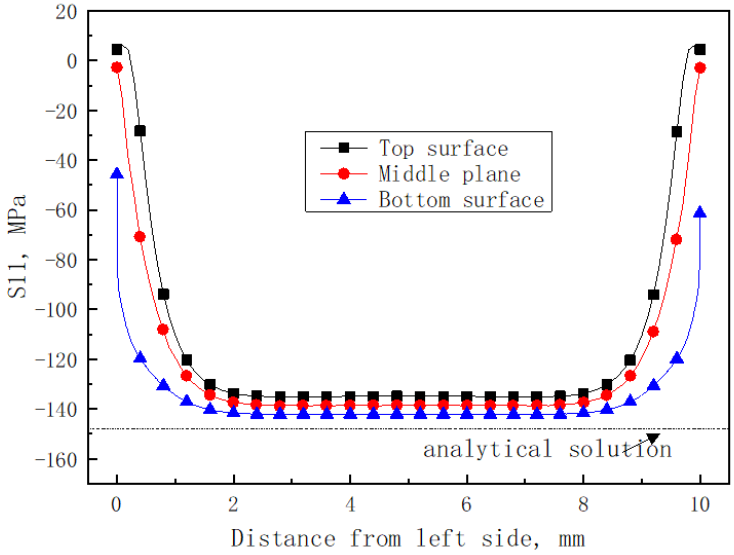

Figure 6. The paths considered in TBC and distributions of S11

The distribution within the TGO is represented in Figure 7. The distribution of stresses is shown in Fig. 7 by selecting the analysis paths similar to σ_{11} within TBC, i.e., the upper and lower surfaces and the three paths in the $h/2$ midplane, respectively. As can be seen in Figure 7, the TGO is all under compressive stress and the stress values are about an order of magnitude higher than those within the TBC, reflecting the singularity of the stresses within the TGO. The distribution of σ_{11} within the TGO is similar to that of σ_{11} within the TBC, with relatively small stress values at the boundary and larger stress values in the middle part, and the stress distribution in the middle part of the TGO is also relatively uniform, with a stress value of about -1.5 GPa in the middle part. The dotted lines in Figure 7 indicate the results of the analytical solution [7]. The stress distribution in the middle part of the TGO is closer to the analytical solution, and the finite element results agree well with the analytical solution if the effect of the boundary is not considered.

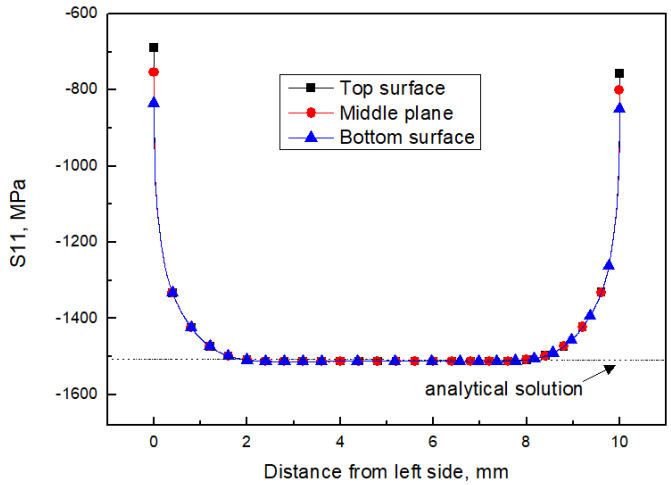

Figure 7. S11 distributions in TGO

Figure 8 represents the distribution of σ_{11} within BC, and the same three paths are selected for the upper and lower surfaces and the h/2 midplane. From the figure, it can be seen that the stress distribution within the BC layer is also uneven. The upper surface at the boundary of the two ends is subject to tensile stress, and the maximum stress value reaches about 325 MPa, the middle surface of h/2 and the lower surface are in a state of compressive stress, and the lower surface of BC has a maximum stress value of about -60 MPa at the boundary. The stress distribution in the middle part is more uniform and the stress values are relatively small, all below 10 MPa. the difference between the stresses on the upper and lower surfaces of BC is small. The dotted lines in the figure indicate the results of the analytical solution [7].

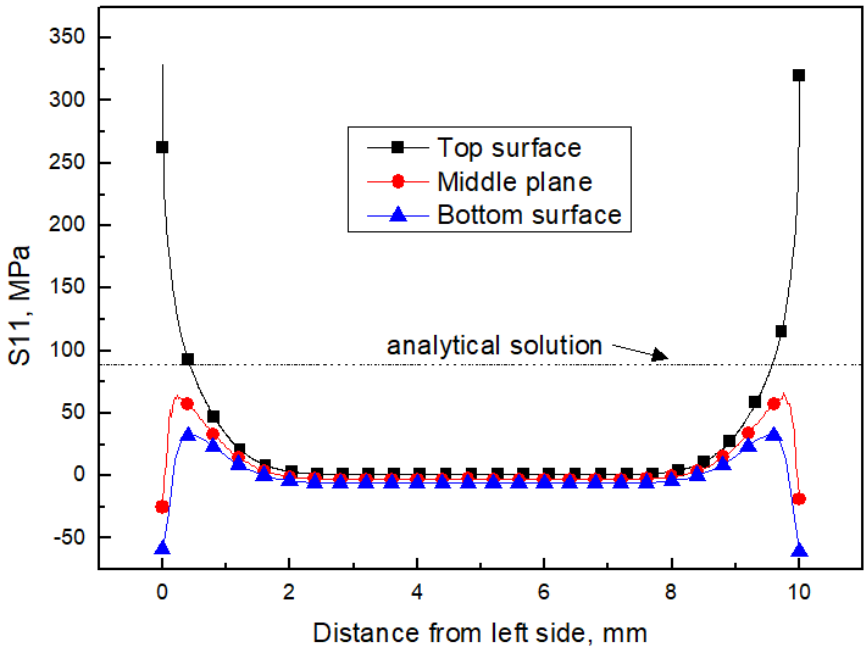

Figure 8. S11 distributions in BC

Figure 9 represents the distribution of σ_{11} within the substrate. Figure 9(a) indicates the selected analysis paths within the substrate, and Figure 9(b) indicates the distribution of σ_{11} on the selected paths. From the figure, it can be seen that the upper surface of the substrate and paths 2 to 4 are mostly in the state of tensile stress, and path 5 and the lower surface are in the state of compressive stress. The stress value on the upper surface of the substrate is the largest, and the stress on path 4 is the smallest, and its size is close to 0 MPa, which is the neutral axis position of the substrate. In all paths, the stresses near the diametral boundary are relatively small, and the stress values in the intermediate parts are relatively large. On the upper surface of the substrate, there is a stress extreme at about 0.5 mm from the diametral boundary, and the stress reaches about 160 MPa. The stress in the middle part of the upper surface of the substrate is about 120 MPa. the stress value in the middle part of the lower surface of the substrate is about -70 MPa. the dotted lines in the figure indicate the results of the analytical solution [7].

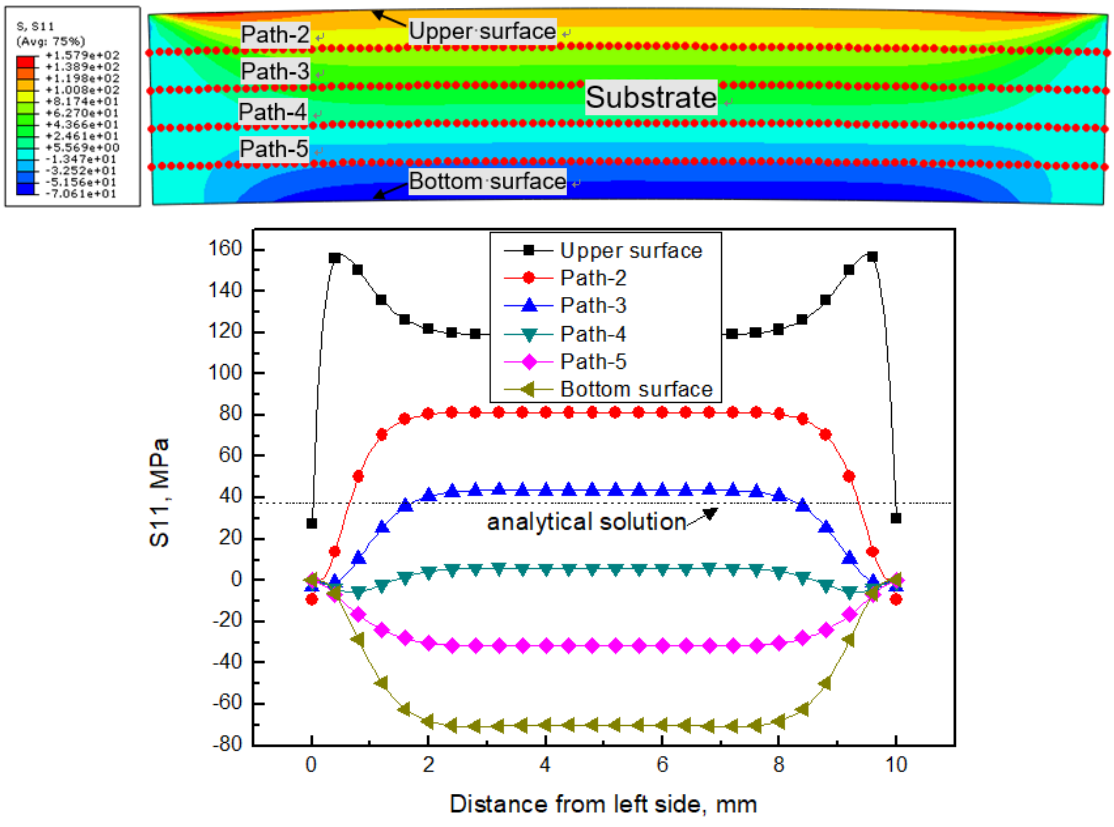

Figure 9. (a) The selected pathes, (b) S11 distributions in substrate

Figure 10 represents the distribution of the stress σ_{22} in the thickness direction within the system. Figure 10(a) represents the distribution cloud of σ_{22} in the system. From the figure, we can see that the stress is more concentrated at the interface of the two sides of the boundary, and the stress distribution is uniform and the stress value is smaller in the middle part which is far from the boundary. One of the important factors contributing to interface cracking is σ_{22}. Figure 10(b) indicates the distribution of σ_{22} at the three interfaces of TBC-TGO, TGO-BC, and BC-base. From Figure 10(b), it can be seen that σ_{22} is in a state of compressive stress at the two-end boundary position, and the stress value is relatively large, reaching about -400 MPa, and the stress in the middle part is relatively small. There is an extreme value of stress at about 0.5 mm from the boundary of the two ends, and the stress value at the interface of TBC-TGO and TGO-BC is about 13 MPa, and the stress value at the interface of BC and substrate reaches about 31 MPa, and the interface cracking may appear in these areas first.

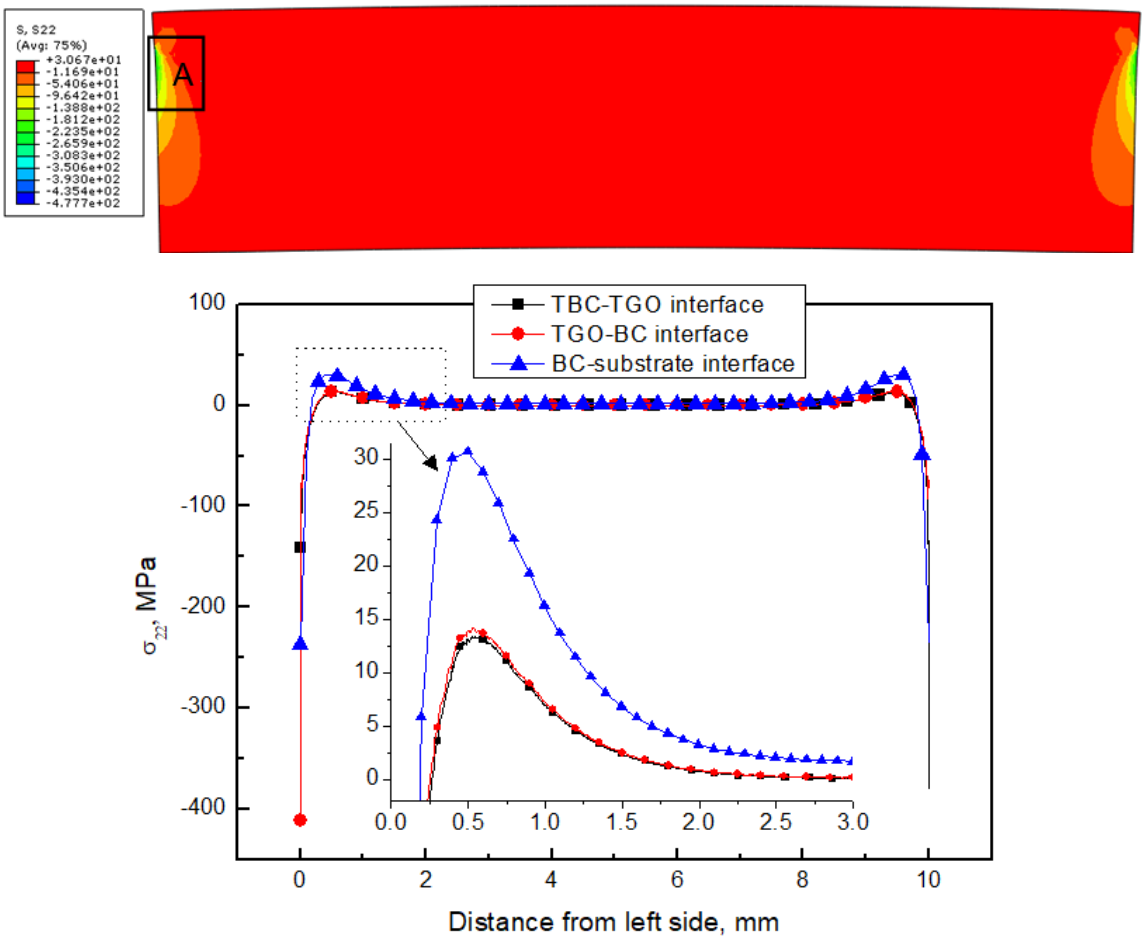

Figure 10. (a) Distributions of S22 (b) S22 of the interface of TBC and TGO

3.2. Effect of Ceramic Layer Thickness Hc on Residual Stress Field

We focus on the effect of TBC thickness h_c on the internal stresses in TBC and TGO. Since the stress distribution within each layer is not uniform, we mainly selected the stress values in the middle part of each layer because the stress distribution in the middle part of the region is uniform and less influenced by the boundary [16]. The preparation temperature was chosen to be 800°C and the ceramic layer thickness h_c was varied from 0.1 mm to 0.9 mm.

Figure 11 represents the stress cloud diagram of σ_{11} under different h_c. From the figure, it can be seen that as h_c increases, the stress level also increases, and the stress distribution in the system also tends to be non-uniform, and the stress gradient in the system increases.

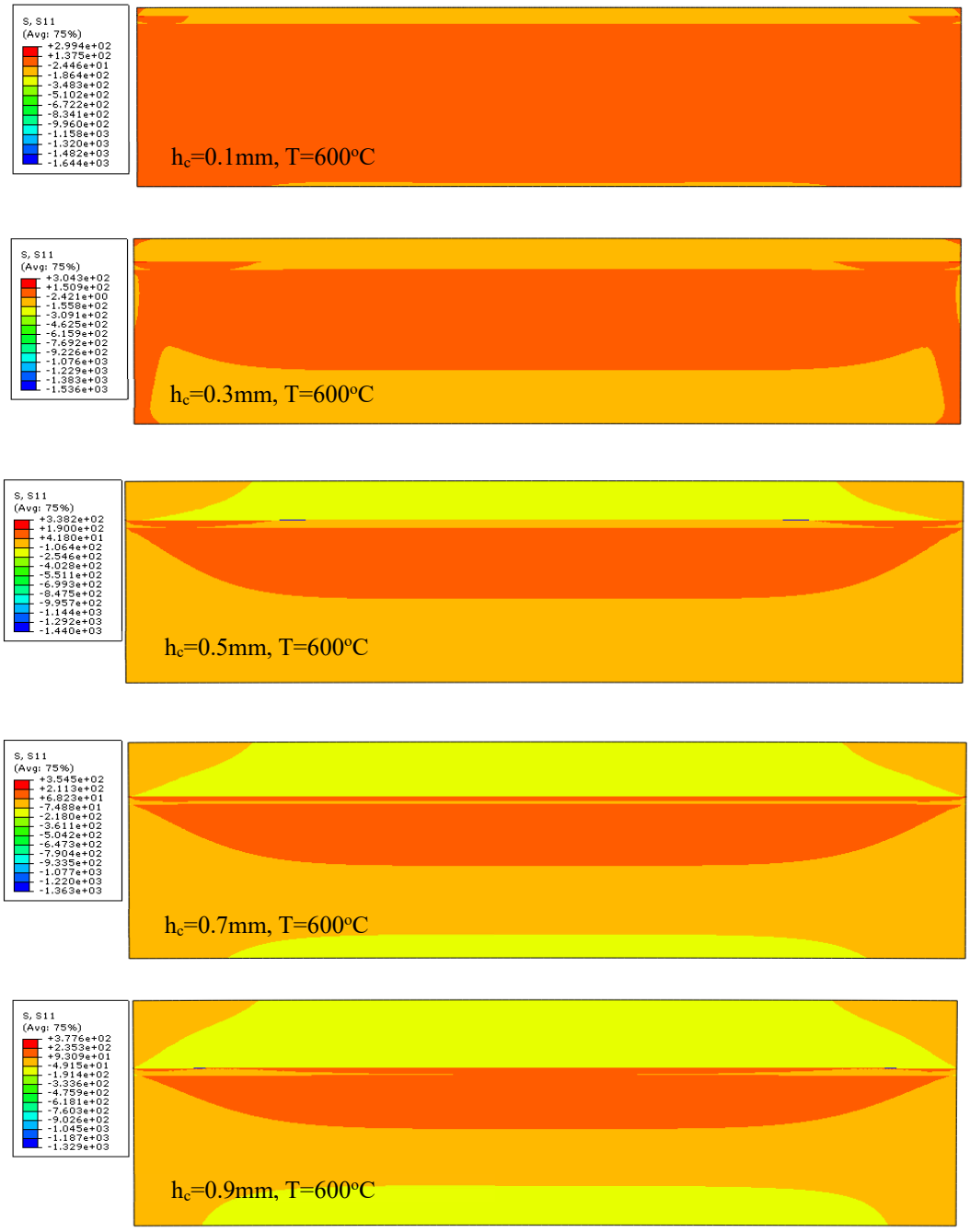

Figure 11. Contours of σ_{11} with different h_c (T=600°C)

Figure 12 represents the effect of ceramic coating spray thickness h_c on the thermal residual stresses within the TBC and TGO after deposition from different preparation temperatures and cooling to room temperature. It can be seen from the figure that the stress values within the TBC and TGO increase with the increase of h_c, which is consistent with the results predicted by the theoretical model [7].

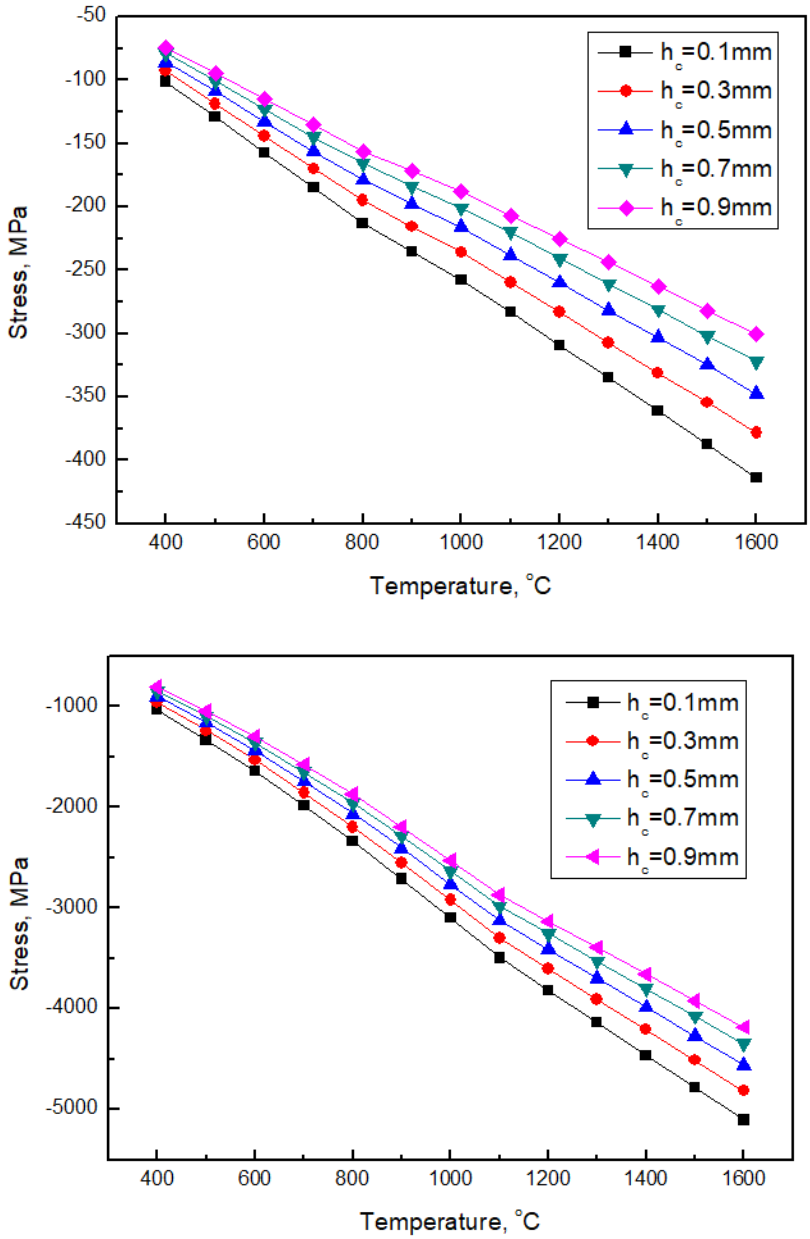

Figure 12. Effects of h_c on the residual stress distribution of TBC (a) and TGO (b)

3.3. Influence of the Thickness h_t of The Oxide Layer Generated During The Preparation Process on The Residual Stress Distribution

The effect of the thickness of TGO formed during the preparation process on the residual stress field within TBC and TGO is shown in Figure 13, from which it can be seen that the residual stress within TBC and TGO increases with the thickness of TGO, but increases very slowly. The influence of the thickness of TGO is relatively large when the preparation temperature is relatively high. This indicates that the thickness of the oxide layer generated during the preparation process has a relatively small effect on the residual stresses within the TBC and TGO. However, during the service of the thermal barrier coating, the increase in the thickness of TGO has a significant effect on the internal stresses in the system and is one of the important causes of coating spalling [1].

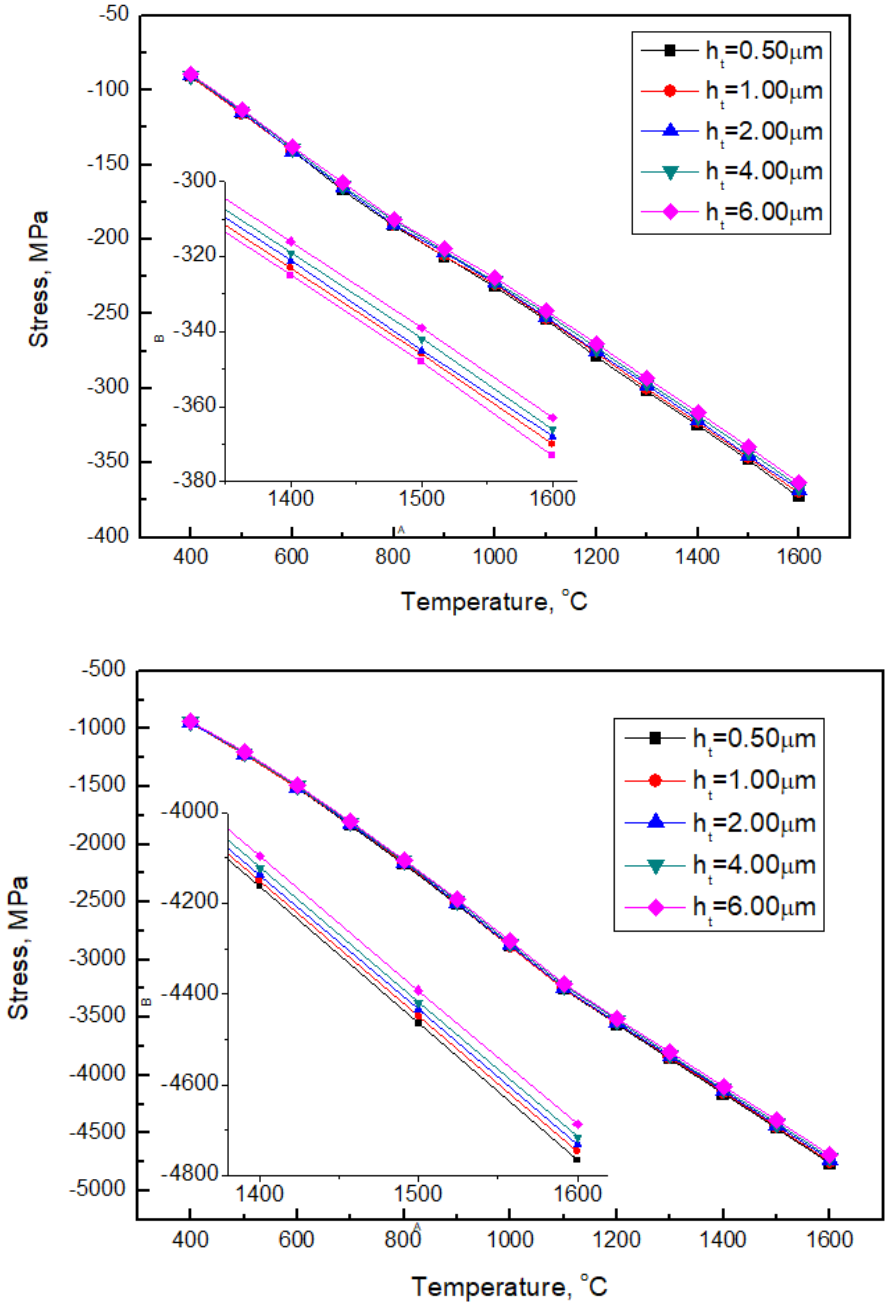

Figure 13. Effects of thickness of TGO on the residual stresses of TBC (a) and TGO (b)

4. Cooling Mode II: Thermal Barrier Coating System Cooling to Room Temperature When There Is A Temperature Gradient

When the thermal barrier coating system is prepared and cooled, assuming the existence of a temperature gradient for each layer, it may be useful to set the TGO, BC and substrate temperatures all fixed at 800°C and the ceramic coating cooled from different temperatures (800°C-1600°C) to room temperature. Figure 14 represents the distribution cloud of the system's displacement in the u_2 direction.

From figure 14, the morphological changes of the system can be seen. As the preparation temperature increases, the bending direction of the thermal barrier coating system gradually bends excessively from the direction of the coating to the direction of the substrate, which is caused by the difference of the thermal expansion coefficients of the layers of materials.

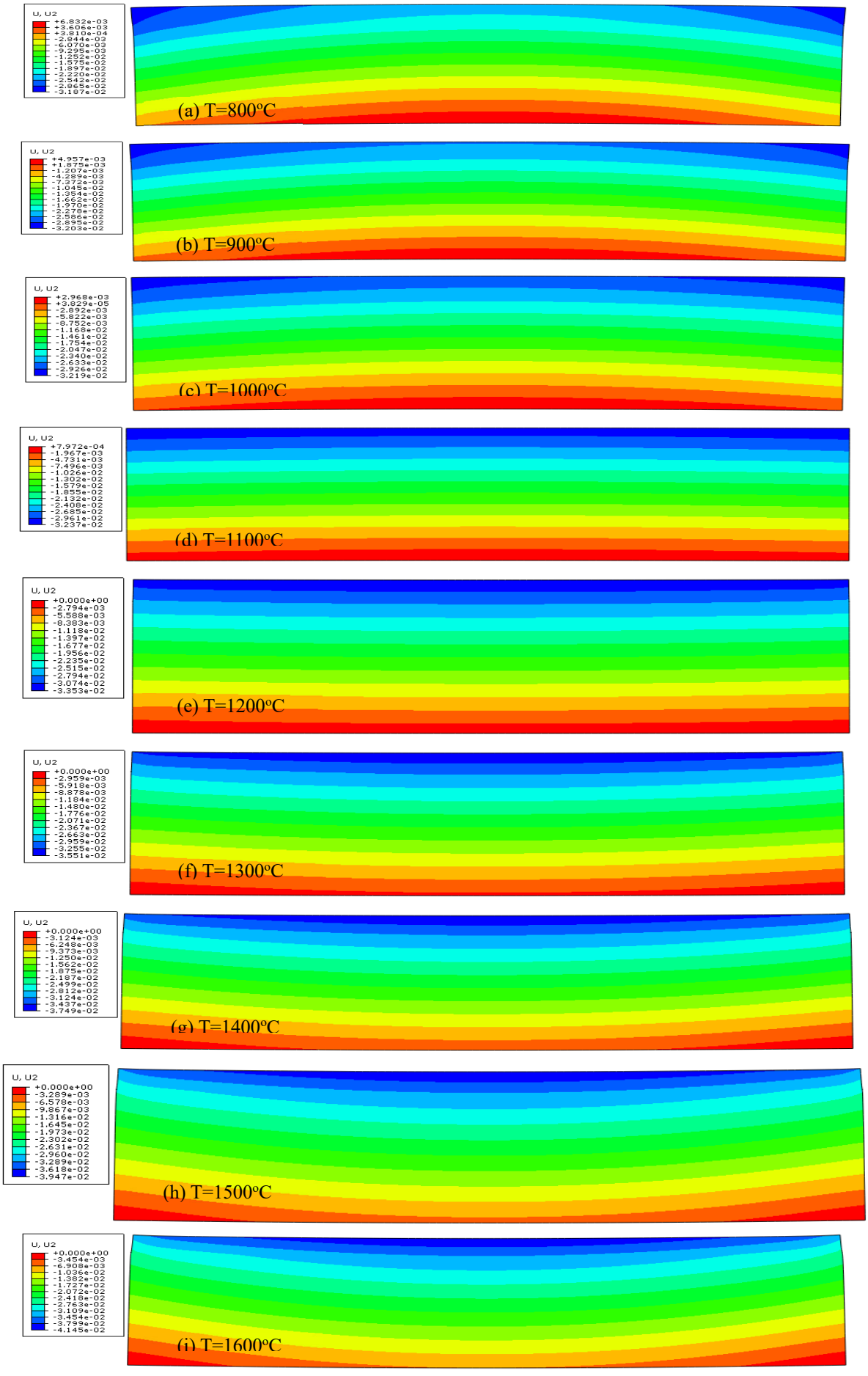

Figure 14. Contours of U2 in TBCs under the condition of temperature gradient

Figure 15 represents the distribution of u_2 on the upper and lower surfaces of the system (i.e., the upper surface of the

TBC and the lower surface of the substrate) at various preparation temperatures. As can be seen in Figure 15(a), the u_2 on the upper surface is negative, and the displacement becomes progressively larger with the increase of the preparation temperature. Figure 15(b) represents the relationship between the substrate lower surface u_2 and the preparation temperature, when the preparation temperature is less than 1100°C, the displacement decreases continuously with the increase of the preparation temperature, and over 1200°C, the displacement becomes negative and increases continuously with the increase of the preparation temperature. That is, the thermal barrier coating system changes from bending in the direction of the coating to bending in the direction of the substrate.

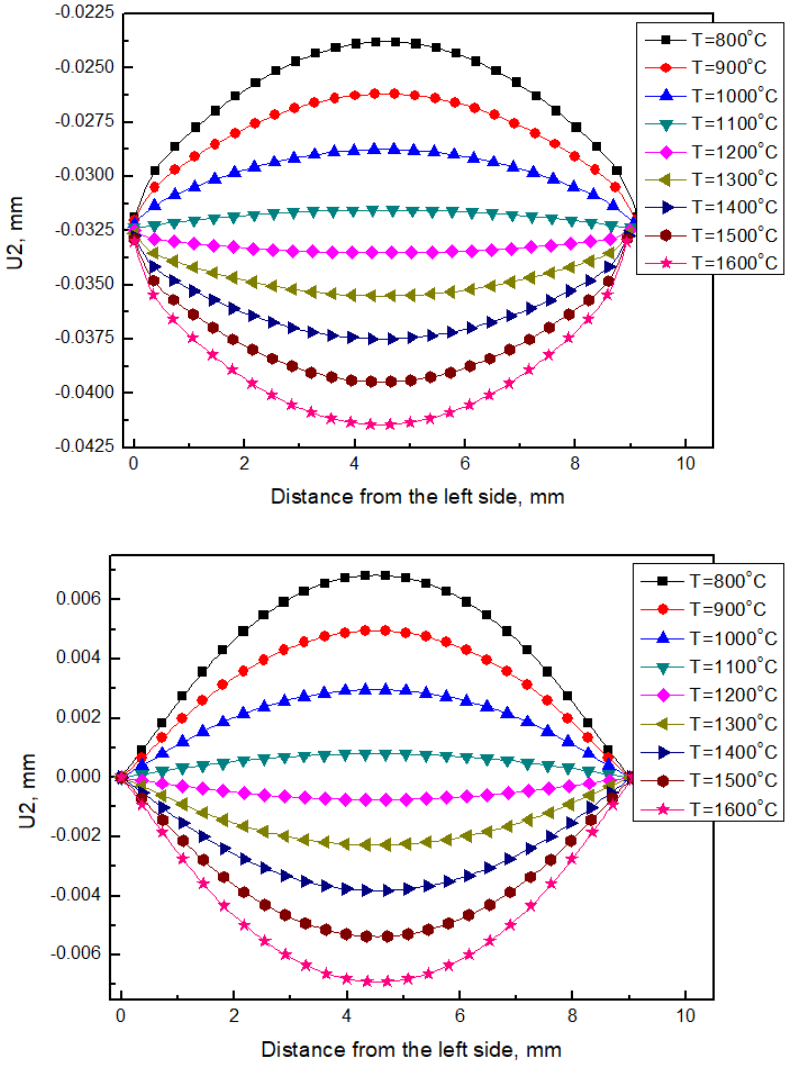

Figure 15. Distributions of U2 (a)top surface and (b)bottom surface

Figure 16 represents the distribution of σ_{11} within the TBC in the presence of a temperature gradient.With the increase of the preparation temperature, the stress gradually oversteps from the state of compressive stress to the state of tensile stress, and the distribution also tends to be uneven, with the stress at the boundary of the two end surfaces being smaller and the stress in the middle part being larger. When the preparation temperature is less than 1100°C, TBC is mainly in the state of compressive stress, and when the preparation temperature is greater than 1100°C, TBC is mainly in the state of tensile stress. When the preparation temperature is 800°C, the stress in the middle part of TBC is about -180MPa, and when the preparation temperature is 1600°C, the stress in the middle part of TBC is about 250MPa. When the preparation temperature is 1100°C, the stress in the middle part of TBC is the smallest, within 5 MPa. Therefore, in the case of considering the temperature gradient, the preparation temperature is chosen to be 1000°C~1100°C to minimize the internal stress in TBC.

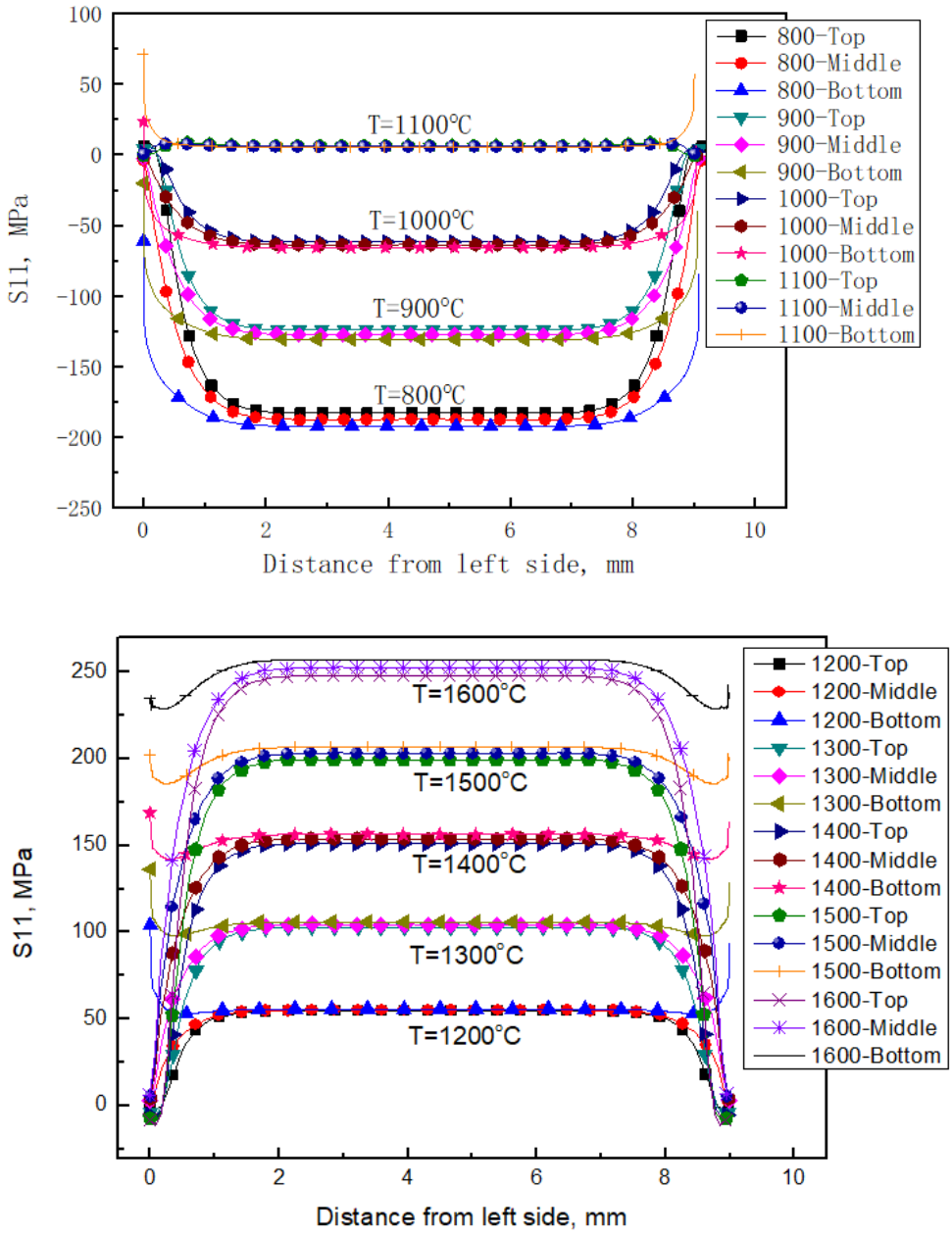

Figure 16. Distributions of S11 in TBC under the condition of temperature gradient

The distribution of σ_{11} within the TGO is shown in Figure 17, from which it can be seen that the stresses within the TGO are the smallest at the boundary and the largest in the middle part at various preparation temperatures, and the distribution is more uniform in the middle part because the middle part is less influenced by the boundary. The higher the preparation temperature, the higher the internal stress in TGO. When the preparation temperature is 800℃, the stress in the middle part of TGO is about -2.1 GPa, and when the preparation temperature is 1600℃, the stress in TGO is about -3.7 GPa. When the preparation temperature is 1600℃, there is a stress singularity at a distance of about 0.4 mm from the boundary, where the stress value is the largest and can be a danger point within the TGO.

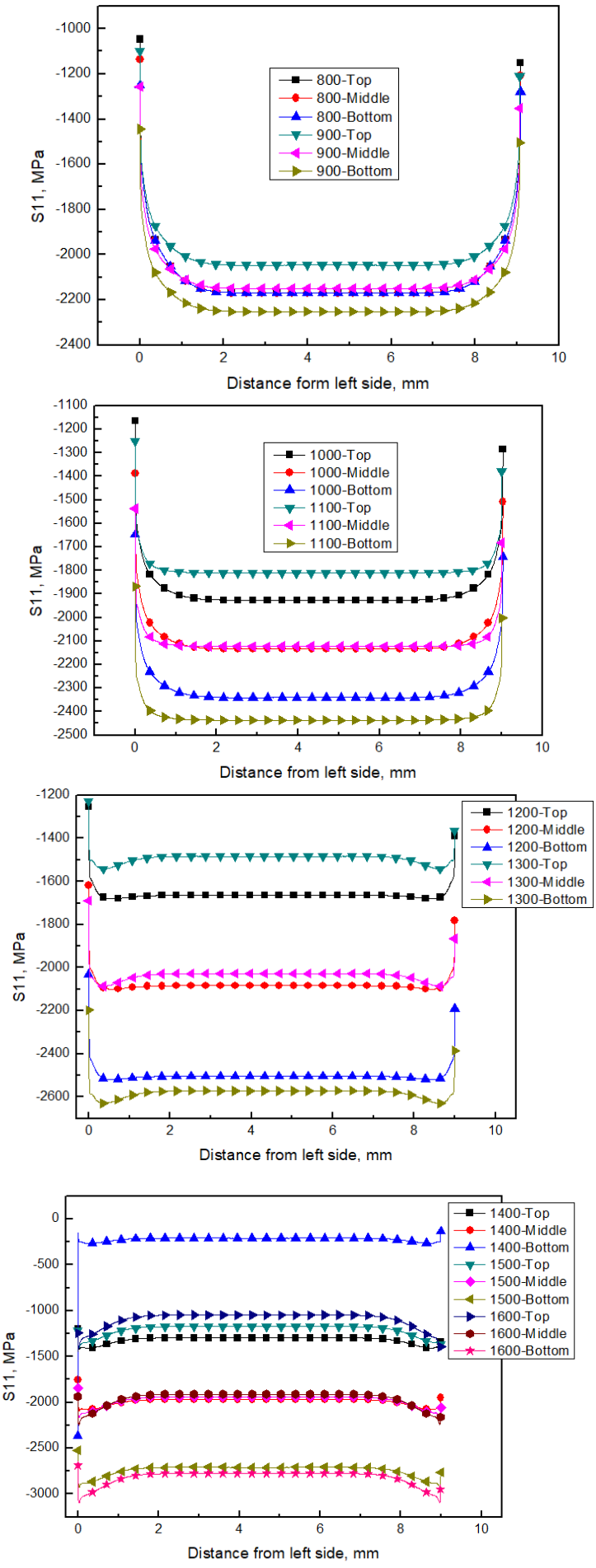

Figure 17. Distributions of S11 in TGO under the condition of temperature gradient

Figure 18 represents the distribution of σ_{11} within BC in the presence of a temperature gradient. The stress is lowest near the boundary, close to 0 MPa. The stress is maximum at about 0.4mm from the boundary, and the stress is uniformly distributed in the middle part. As the preparation temperature increases, the stress distribution within the BC layer gradually changes mainly from tensile stress to compressive stress. When the preparation temperature is 1200℃, the stress in the middle part within the BC is about 120 MPa, and when the preparation temperature is 1600℃, the stress within the BC is about -270 MPa.

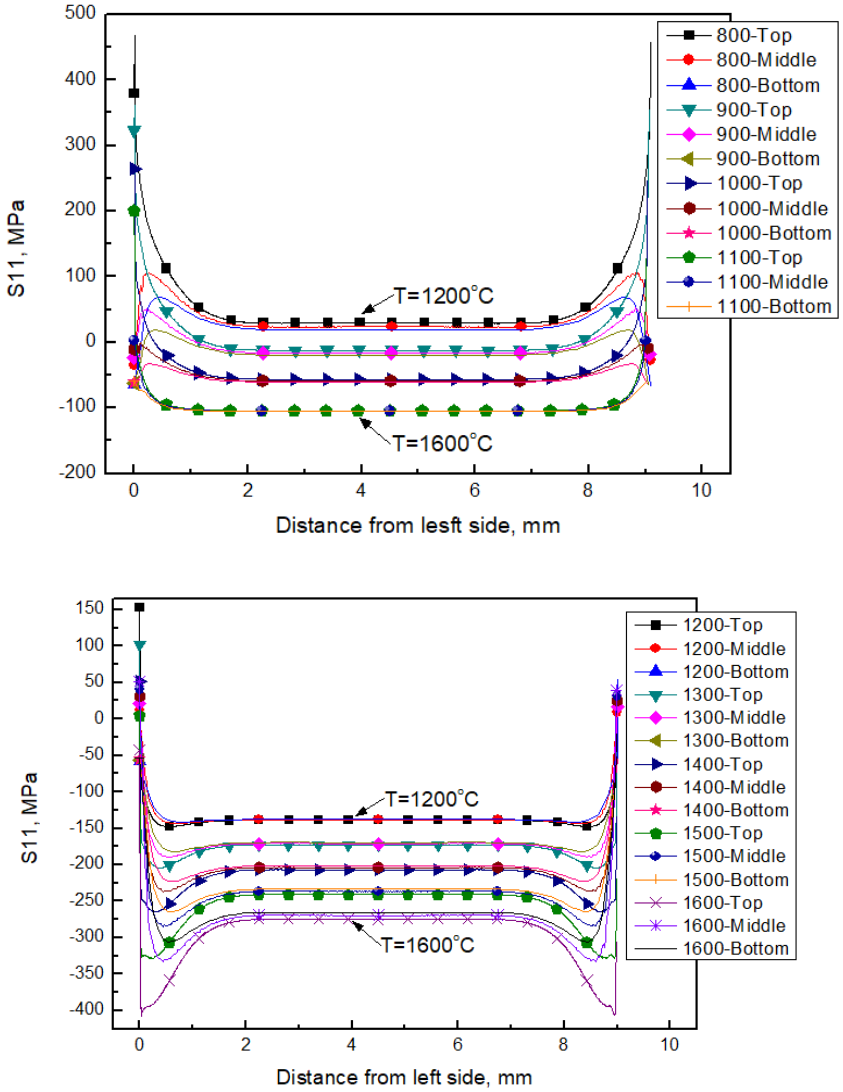

Figure 18. Distributions of S11 in BC under the condition of temperature gradient

Figure 19 represents the distribution of σ_{11} within the substrate in the presence of a temperature gradient. The stress near the boundary is the smallest, and the middle part is larger and tends to be uniform. The stress in the substrate near the top within the substrate decreases as the preparation temperature increases and gradually shifts to a state of compressive stress, with the stress in the middle part within path 1 being about 160 MPa when the preparation temperature is 800℃ and about -125 MPa. When the preparation temperature is 1600 ℃. The stress in the part of the substrate near the bottom decreases with the increase of the preparation temperature and gradually shifts to a state of tensile stress. When the preparation temperature is 800 ℃, the stress in the middle part of path 5 is about -40 MPa, and when the preparation temperature is 1600 ℃, the stress is about 40 MPa.

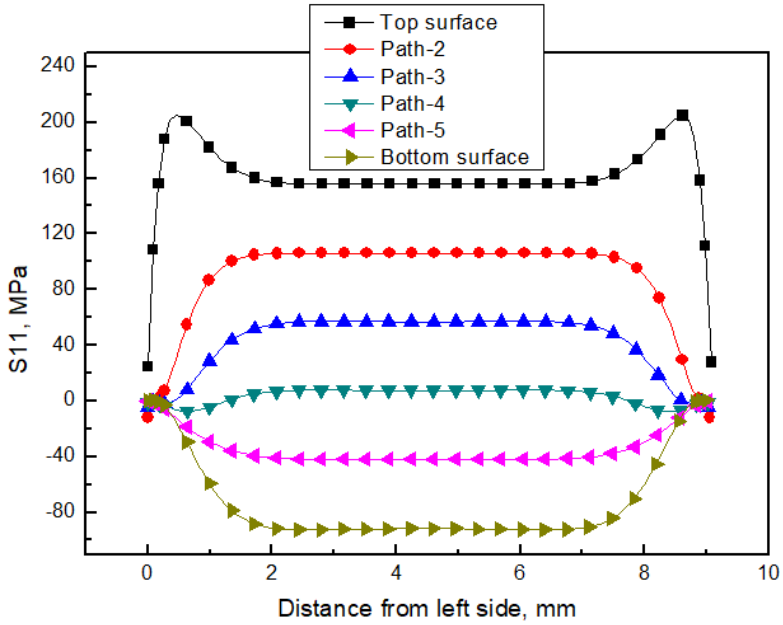

Figure 19. Distributions of S11 in substrate under the condition of temperature gradient

5. Conclusion

(1) When the flat plate thermal barrier coating system is uniformly cooled from the preparation temperature to room temperature, residual stresses exist in each layer, within the TBC is the residual compressive stress, when h_c=0.35mm, within the set preparation temperature range, its size is approximately between 0 to -140MPa, the residual compressive stress within the TGO is particularly large, about 0.9 to 1 GPa change, the layer exists stress singularity is the cause of thermal barrier coating failure The stress singularity in this layer is the main reason for the failure of the thermal barrier coating, which eventually leads to the generation of damage such as delamination, spalling and buckling of the ceramic coating. The distribution of residual stresses in the substrate and BC is more complex and varies with the temperature at which deposition is first initiated.

(2) It was found by calculation that as the thickness of the sprayed ceramic powder increased, the residual stresses within the TBC and TGO all tended to decrease, and the overall buckling phenomenon tended to become apparent.

(3) The thickness of the TGO generated during the preparation process does not have a significant effect on the distribution of stresses within the TBC and TGO.

(4) When cooling in the presence of temperature gradient conditions, the deformation of the system is not consistent at different preparation temperatures. When the preparation temperature is less than 1200℃ the system bends mainly in the direction of the coating, and when the preparation temperature is greater than 1200℃, the system bends mainly in the direction of the substrate. The initial residual stress within the TBC is minimized when the preparation temperature is in the range of 1000℃ to 1100℃.

References

[1] N. P. Padture, M. Gell, E. H. Jordan, Thermal Barrier Coatings for Gas-Turbine Engine Applications. Science, 2002, 296: 280-284.

[2] R. A. Miller, Current status of thermal barrier coatings-an overview. Surface and Coatings Technology, 1987, 30: 1-11.

[3] R. A. Miller, Thermal barrier coatings for aircraft engines: history and directions. Journal of Thermal Spray Technology, 1997, 6（1）: 35-42.

[4] S. M. Meier, D. K. Gupta, The Evolution of Thermal Barrier Coating in Gas Turbine Engine Applications. Journal of Engineering for Gas Turbines and Power, 1994, 116: 250-257.

[5] X. G. Yang，R. Gen, C. B. Xiong, A simple method for residual stress analysis of thermal insulation coating and Discussion on the results, Journal of Aerospace Power, 1997, 12（3）: 239-142.

[6] D. F. Yang, S. Han, W. Yuan, Study on the influences of the substrate preheating temperature on the thermal residual stress of the thermal barrier coating, Surface Technology, 2004, 33（2）: 22-28.

[7] W. G. Mao, C. Y. Dai, Y. C. Zhou, Prediction of qresidual stress in thermal barrier coating during the deposition process, 2005, 27(4): 46-52.

[8] V. Teixeira, M. Andritschky, H. P. Buchkremer, D. Stöver, Effects of deposition temperature and thermal cycling on residual stress state in zirconia-based thermal barrier coatings. Surface and Coatings Technology, 1999, 120: 103-111.

[9] J. H. Harding, P. A. Mulheran, S. Cirolini, M. Marchese, G. Jacucci, Modeling the deposition process of thermal barrier coatings. Journal of Thermal Spray Technology, 1995, 4（1）:34-40.

[10] V. Teixeira, Mechanical integrity in PVD coatings due to the presence of residual stresses. Thin Solid Films, 2001, 392: 276-281.

[11] S. Widjaja, A. M. Limarga, T. H. Yip, Modeling of residual stresses in a plasma-sprayed zirconia/alumina functionally graded-thermal barrier coating. Thin Solid Films, 2003, 434: 216-227.

[12] A. Rabiei, A. G. Evans, Failure mechanisms associated with the thermally grown oxide in plasma-sprayed thermal barrier coatings. Acta Materialia, 2000, 48: 3963-3976.

[13] S. Sridharan, L. Xie, E. H. Jordan, M. Gell, Stress variation with thermal cycling in the thermally grown oxide of an EB-PVD thermal barrier coating. Surface and Coatings Technology, 2004, 179（2）: 286-296.

[14] Y. C. Zhou, T. Hashida, Thermal fatigue failure induced by delamination in thermal barrier coating. International Journal of Fatigue, 2002, 24: 407-417.

[15] W. G. Mao, Y. C. Zhou, L. Yang, X. H. Yu, Modeling of residual stresses variation with thermal cycling in thermal barrier coating. Mechanics of Materials, 2006, 38: 1118-1127.

[16] J. Haidera, M. Rahmana, B. Corcoranb, M. S. J. Hashmia, Simulation of thermal stress in magnetron sputtered thin coating by finite element analysis. Journal of Materials Processing Technology, 2005, 168: 36-41.